Antebas, A.; Denia, F.D.; Pedrosa, A.; Fuenmayor, F. (2013). A finite element approach for the acoustic modelling of perforated dissipative mufflers with non-homogeneous properties. Mathematical and Computer Modelling. 57(7):1970-1978. doi:10.1016/j.mcm.2012.01.021.

A finite element approach for the acoustic modelling of perforated dissipative mufflers with non-homogeneous properties.

A.G. Antebas, F.D. Denia*, A.M. Pedrosa, F.J. Fuenmayor

Centro de Investigación de Tecnología de Vehículos, Universitat Politècnica de València, Camino de Vera s/n, 46022 Valencia, Spain.

Abstract

In this work, a finite element approach is presented for modelling sound propagation in perforated dissipative mufflers with non-homogeneous properties. The spatial variations of the acoustic properties can arise, for example, from uneven filling processes during manufacture and degradation associated with the flow of soot particles within the absorbent material. First, the finite element method is applied to the wave equation for a propagation medium with variable properties (outer chamber with absorbent material) and a homogeneous medium (central passage). For the case of a dissipative muffler, the characterization of the absorbent material is carried out by means of its equivalent complex density and speed of sound. To account for the spatial variations of these properties, a coordinate-dependent function is proposed for the filling density of the absorbent material. The coupling between the outer chamber and the central passage is achieved by using the acoustic impedance of the perforated central pipe, that relates the acoustic pressure jump and the normal velocity through the perforations. The acoustic impedance of the perforated central duct includes the influence of the absorbent material and therefore a spatial variation of the impedance is also taken into account. A detailed study is then presented to assess the influence of the heterogeneous properties and the perforated duct porosity on the acoustic attenuation performance of the muffler.

Keywords: heterogeneous absorbent material, muffler, finite element approach, variable filling density

1. Introduction

Due to their broadband characteristics at mid to high frequencies, the dissipative mufflers have been widely used in vehicle exhaust systems. Although plane wave models [1] are available for the prediction of the sound attenuation of mufflers at low frequency, multidimensional analytical techniques [2–4] and numerical methods [5–10] are required for higher frequencies and to consider, for example, the propagation of higher order modes. While multidimensional analytical methods are desirable due to their low computational effort, they are not capable to

*Corresponding author. Tel.: +34 963877007 Ext: 76225; fax: +34 963877629.
Email address: fdenia@mcm.upv.es (F.D. Denia)

model complex silencer geometries or non-homogeneous properties. For this reason, numerical techniques have found favour for modelling complex geometries and arbitrary boundary conditions. Among the numerical methods, the finite element method (FEM) is widely used and relevant literature can be found regarding the acoustic modelling of silencers. Young and Crocker [5] applied the finite element method to reactive concentric expansion silencers to predict their transmission loss. Kagawa *et al.* [11] and Craggs [12] studied the transmission loss of a lined expansion muffler assuming a locally reacting effect of the absorbent material. Finite element models for bulk reacting absorbent materials were presented by Kirby to consider perforated dissipative mufflers with homogeneous properties [13, 14]. Elnady *et al.* [15] used the finite element method to validate their proposed approach for modelling perforated pipes.

In the previous works, the absorbent materials considered were assumed to be homogeneous. However, in realistic cases of automotive silencers, this assumption is not always fulfilled and heterogeneous acoustic properties of the fibrous materials appear. The presence of these non-homogeneous properties may arise, for example, from uneven filling processes in dissipative mufflers [2, 16] and degradation produced by the flow of soot particles within the absorbent material [17]. These two phenomena can cause significant variation in the filling density of the fibrous material, which as a consequence leads to heterogeneity of its equivalent complex density and speed of sound. To the authors' knowledge, the only reference in the literature that tried to model dissipative mufflers with heterogeneous fibrous material was the work of Peat and Rathi [6]. In this case, the heterogeneity was associated with the mean flow induced in the absorbent material.

In Ref. [6] no perforated duct was considered and the fibrous material was exposed directly to the gas in the central airway. However, in the automotive silencers, a perforated screen is usually placed to protect the fibrous material and to reduce static pressure losses over the silencer. The acoustic impedance of a perforated surface in absence of absorbent material was studied by Sullivan and Crocker [18]. Kirby and Cummings [19] obtained a semiempirical relationship for the acoustic impedance of perforated plates with a porous material backing the perforations, which depends upon various parameters including the equivalent complex density. Futher investigations were carried out by Lee *et al.* [20] to account for the influence of the absorbent propagation medium on acoustic behaviour of the perforated screen. When the bulk reacting material in contact with the perforations is considered to be homogeneous, the acoustic impedance of the perforated plate is constant from a spatial point of view [3, 4, 21]. However, in the case of non-homogeneous porous backing material, a modified expression of the acoustic impedance must be regarded to account for the spatial coordinate dependence of the equivalent properties.

2. Mathematical approach

2.1. Finite element formulation

Figure 1 shows the perforated dissipative muffler studied in this work, which consists of a perforated duct surrounded by a non-homogeneous absorbent material. The subdomains of the central airway and the absorbent material are denoted by Ω_a and Ω_m, respectively, while Γ_a and Γ_m represent their boundary surfaces which are supposed to satisfy the rigid wall boundary condition [1], except for the inlet and outlet sections Γ_i and Γ_o and the perforated duct surface Γ_p. The central passage with air is characterized by the density ρ_0 and the speed of sound c_0, while its perforated surface is considered by means of the acoustic impedance $\tilde{Z}_p$. To account for the heterogeneous properties of the absorbent material, the equivalent complex density $\rho_m(\mathbf{x})$ and

speed of sound $c_m(\mathbf{x})$ [22] are coordinate-dependent, which leads to spatial variations of $\tilde{Z}_p(\mathbf{x})$ as well. Further details will be provided in Sec. 2.2 and 2.3.

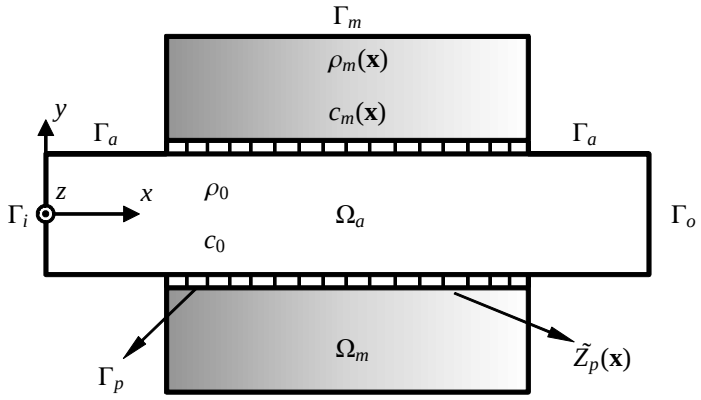

Figure 1: Perforated dissipative silencer with heterogeneous absorbent material.

For the central airway, the wave propagation is governed by the well-known Helmholtz equation [1],

$$\nabla^2 P_a + k_0^2 P_a = 0 \tag{1}$$

with ∇^2 being the Laplacian operator, P_a the acoustic pressure and k_0 the wavenumber in the air, defined as the ratio of the angular frequency ω to the speed of sound c_0.

In the heterogeneous absorbent material, the wave propagation is given by the equation [23],

$$\nabla\left(\frac{1}{\rho_m}\nabla P_m\right) + \frac{1}{\rho_m}k_m^2 P_m = 0 \tag{2}$$

where $k_m(\mathbf{x}) = \omega/c_m(\mathbf{x})$ is the equivalent complex wavenumber associated with the heterogeneous absorbent material.

By using the finite element method, the acoustic pressure within element e of the silencer is approximated by trial functions [24], which leads to

$$P_a = \sum_{i=1}^{N_{npe}} N_i \tilde{P}_{a_i}^e = \mathbf{N}\tilde{\mathbf{P}}_a^e \tag{3}$$

$$P_m = \sum_{i=1}^{N_{npe}} N_i \tilde{P}_{m_i}^e = \mathbf{N}\tilde{\mathbf{P}}_m^e \tag{4}$$

where $\tilde{P}_{a_i}^e$ and $\tilde{P}_{m_i}^e$ are the nodal pressures, N_i are the shape functions and N_{npe} is the number of nodes per element. By applying the method of weighted residuals in combination with the Galerkin approach [24], and after using Green's theorem, the weighted residual associated with the subdomain Ω_a can be written as

$$\sum_{e=1}^{N_e^a}\left(\int_{\Omega_a^e}\nabla^{\mathrm{T}}\mathbf{N}\nabla\mathbf{N}\mathrm{d}\Omega-k_0^2\int_{\Omega_a^e}\mathbf{N}^{\mathrm{T}}\mathbf{N}\mathrm{d}\Omega\right)\tilde{\mathbf{P}}_a^e=\sum_{e=1}^{N_e^a}\int_{\Gamma_a^e}\mathbf{N}^{\mathrm{T}}\frac{\partial P_a}{\partial n}\mathrm{d}\Gamma \tag{5}$$

and the weighted residual of subdomain Ω_m is

$$\sum_{e=1}^{N_e^m}\left(\int_{\Omega_m^e}\frac{1}{\rho_m}\nabla^{\mathrm{T}}\mathbf{N}\nabla\mathbf{N}\mathrm{d}\Omega-\int_{\Omega_m^e}\frac{k_m^2}{\rho_m}\mathbf{N}^{\mathrm{T}}\mathbf{N}\mathrm{d}\Omega\right)\tilde{\mathbf{P}}_m^e=\sum_{e=1}^{N_e^m}\int_{\Gamma_m^e}\frac{1}{\rho_m}\mathbf{N}^{\mathrm{T}}\frac{\partial P_m}{\partial n}\mathrm{d}\Gamma \tag{6}$$

where N_e^a and N_e^m are the number of finite elements in the central perforated duct and the absorbent material subdomains, respectively, and n is the outward unit vector.

As the rigid wall condition is satisfied at the boundary $\Gamma_a-\Gamma_p-\Gamma_i-\Gamma_o$, the right side integral of Eq. (5) is only taken over the perforated duct boundary Γ_p and the inlet and outlet surfaces, denoted by Γ_i and Γ_o, respectively. To evaluate the contribution of the perforated boundary Γ_p on the surface integral, the relation that defines the acoustic impedance of the perforated duct must be taken into account [1]. By using the Euler's equation, the normal pressure gradient at the perforated surface in the central airway can be expressed as,

$$\frac{\partial P_a}{\partial n}=-\rho_0\frac{\partial U_{n_a}}{\partial t}=-j\rho_0\omega U_{n_a} \tag{7}$$

U_{n_a} being the acoustic velocity normal to the perforations at the interface.

The acoustic impedance of the perforated surface is defined as the ratio of the acoustic pressure jump across the perforations to the normal acoustic velocity, and can be written as,

$$\tilde{Z}_p=\frac{P_a-P_m}{U_{n_a}} \tag{8}$$

After substituting Eq. (8) into Eq. (7), the normal pressure gradient associated with the perforated duct in the central airway is expressed as

$$\frac{\partial P_a}{\partial n}=-j\rho_0\omega\frac{P_a-P_m}{\tilde{Z}_p} \tag{9}$$

Introducing Eqs. (3) and (4) into Eq. (9), yields for element e

$$\frac{\partial P_a}{\partial n}=-j\rho_0\omega\frac{\mathbf{N}\tilde{\mathbf{P}}_a^e-\mathbf{N}\tilde{\mathbf{P}}_m^e}{\tilde{Z}_p} \tag{10}$$

A similar procedure is applied to calculate the right side integral of Eq. (6). In this case, only the contribution of the perforated boundary Γ_p is computed. By considering Euler's equation, the normal pressure gradient at the perforated surface in the heterogeneous absorbent material is given by

$$\frac{\partial P_m}{\partial n}=-\rho_m\frac{\partial U_{n_m}}{\partial t}=-j\rho_m\omega U_{n_m} \tag{11}$$

where U_{n_m} is the normal velocity at the interface. Considering the continuity of the normal particle velocity and taking into account that the outward unit vectors in the direction normal to the interface of both regions are opposite, the relation ($U_{n_a}=-U_{n_m}$) is satisfied [25], which yields

$$\frac{\partial P_m}{\partial n} = j\rho_m\omega\frac{P_a - P_m}{\tilde{Z}_p} \tag{12}$$

Substituting the trial solutions expressed by Eqs. (3) and (4) into Eq. (12), gives

$$\frac{\partial P_m}{\partial n} = j\rho_m\omega\frac{\mathbf{N}\tilde{\mathbf{P}}_a^e - \mathbf{N}\tilde{\mathbf{P}}_m^e}{\tilde{Z}_p} \tag{13}$$

Replacing the normal pressure gradient in Eq. (5) by Eq. (10), yields

$$\begin{aligned}\sum_{e=1}^{N_e^a}\left(\int_{\Omega_a^e}\nabla^{\mathrm{T}}\mathbf{N}\nabla\mathbf{N}\mathrm{d}\Omega - k_0^2\int_{\Omega_a^e}\mathbf{N}^{\mathrm{T}}\mathbf{N}\mathrm{d}\Omega\right)\tilde{\mathbf{P}}_a^e = \sum_{e=1}^{N_e^a}\int_{\Gamma_a^e\cap\Gamma_i}\mathbf{N}^{\mathrm{T}}\frac{\partial P_a}{\partial n}\mathrm{d}\Gamma \\ + \sum_{e=1}^{N_e^a}\int_{\Gamma_a^e\cap\Gamma_o}\mathbf{N}^{\mathrm{T}}\frac{\partial P_a}{\partial n}\mathrm{d}\Gamma - j\rho_0\omega\sum_{e=1}^{N_e^a}\int_{\Gamma_a^e\cap\Gamma_p}\frac{1}{\tilde{Z}_p}\mathbf{N}^{\mathrm{T}}\left(\mathbf{N}\tilde{\mathbf{P}}_a^e - \mathbf{N}\tilde{\mathbf{P}}_m^e\right)\mathrm{d}\Gamma\end{aligned} \tag{14}$$

where the integrals over Γ_i and Γ_o are associated with the usual excitation boundary conditions [1] and the integral over Γ_p represents a coupling term between Ω_a and Ω_m.

Similarly, after substituting Eq. (13) into Eq. (6), the weighted residual related to the heterogeneous absorbent material subdomain is expressed as

$$\begin{aligned}\sum_{e=1}^{N_e^m}\left(\int_{\Omega_m^e}\frac{1}{\rho_m}\nabla^{\mathrm{T}}\mathbf{N}\nabla\mathbf{N}\mathrm{d}\Omega - \int_{\Omega_m^e}\frac{k_m^2}{\rho_m}\mathbf{N}^{\mathrm{T}}\mathbf{N}\mathrm{d}\Omega\right)\tilde{\mathbf{P}}_m^e = \\ j\omega\sum_{e=1}^{N_e^m}\int_{\Gamma_m^e\cap\Gamma_p}\frac{1}{\tilde{Z}_p}\mathbf{N}^{\mathrm{T}}\left(\mathbf{N}\tilde{\mathbf{P}}_a^e - \mathbf{N}\tilde{\mathbf{P}}_m^e\right)\mathrm{d}\Gamma\end{aligned} \tag{15}$$

To get a more compact form of Eq. (14) associated with the airway subdomain, the following matrices have been defined

$$\mathbf{K}_a = \sum_{e=1}^{N_e^a}\int_{\Omega_a^e}\nabla^{\mathrm{T}}\mathbf{N}\nabla\mathbf{N}\mathrm{d}\Omega \tag{16}$$

$$\mathbf{M}_a = \frac{1}{c_0^2}\sum_{e=1}^{N_e^a}\int_{\Omega_a^e}\mathbf{N}^{\mathrm{T}}\mathbf{N}\mathrm{d}\Omega \tag{17}$$

$$\mathbf{C}_{aa} = \rho_0\sum_{e=1}^{N_e^a}\int_{\Gamma_a^e\cap\Gamma_p}\frac{1}{\tilde{Z}_p}\mathbf{N}^{\mathrm{T}}\mathbf{N}\mathrm{d}\Gamma \tag{18}$$

$$\mathbf{C}_{am} = -\rho_0\sum_{e=1}^{N_e^a}\int_{\Gamma_a^e\cap\Gamma_p}\frac{1}{\tilde{Z}_p}\mathbf{N}^{\mathrm{T}}\mathbf{N}\mathrm{d}\Gamma \tag{19}$$

$$\mathbf{F}_a = \sum_{e=1}^{N_e^a}\int_{\Gamma_a^e\cap\Gamma_i}\mathbf{N}^{\mathrm{T}}\frac{\partial P_a}{\partial n}\mathrm{d}\Gamma + \sum_{e=1}^{N_e^a}\int_{\Gamma_a^e\cap\Gamma_o}\mathbf{N}^{\mathrm{T}}\frac{\partial P_a}{\partial n}\mathrm{d}\Gamma \tag{20}$$

that leads, after some operations, to

$$\left(\mathbf{K}_a + j\omega\mathbf{C}_{aa} - \omega^2\mathbf{M}_a\right)\tilde{\mathbf{P}}_a + j\omega\mathbf{C}_{am}\tilde{\mathbf{P}}_m = \mathbf{F}_a \tag{21}$$

Regarding Eq. (15) the following notation is introduced

$$\mathbf{K}_m = \sum_{e=1}^{N_e^m} \int_{\Omega_m^e} \frac{1}{\rho_m} \nabla^{\mathrm{T}}\mathbf{N}\nabla\mathbf{N}\mathrm{d}\Omega \tag{22}$$

$$\mathbf{M}_m = \sum_{e=1}^{N_e^m} \int_{\Omega_m^e} \frac{1}{\rho_m}\frac{1}{c_m^2}\mathbf{N}^{\mathrm{T}}\mathbf{N}\mathrm{d}\Omega \tag{23}$$

$$\mathbf{C}_{ma} = -\sum_{e=1}^{N_e^m} \int_{\Gamma_m^e \cap \Gamma_p} \frac{1}{\tilde{Z}_p}\mathbf{N}^{\mathrm{T}}\mathbf{N}\mathrm{d}\Gamma \tag{24}$$

$$\mathbf{C}_{mm} = \sum_{e=1}^{N_e^m} \int_{\Gamma_m^e \cap \Gamma_p} \frac{1}{\tilde{Z}_p}\mathbf{N}^{\mathrm{T}}\mathbf{N}\mathrm{d}\Gamma \tag{25}$$

Now Eq. (15) can be expressed in the following compact form

$$\left(\mathbf{K}_m + j\omega\mathbf{C}_{mm} - \omega^2\mathbf{M}_m\right)\tilde{\mathbf{P}}_m + j\omega\mathbf{C}_{ma}\tilde{\mathbf{P}}_a = \mathbf{0} \tag{26}$$

Gauss quadrature integration is used to evaluate integrals Eqs. (16)-(19) and Eqs. (22)-(25). Special attention must be paid to include accurately the spatial variations of the heterogeneous properties ρ_m, c_m and $\tilde{Z}_p$.

Finally, Eqs. (21) and (26) can be written in matrix form as

$$\left(\begin{bmatrix}\mathbf{K}_a & \mathbf{0}\\ \mathbf{0} & \mathbf{K}_m\end{bmatrix} + j\omega\begin{bmatrix}\mathbf{C}_{aa} & \mathbf{C}_{am}\\ \mathbf{C}_{ma} & \mathbf{C}_{mm}\end{bmatrix} - \omega^2\begin{bmatrix}\mathbf{M}_a & \mathbf{0}\\ \mathbf{0} & \mathbf{M}_m\end{bmatrix}\right)\begin{Bmatrix}\tilde{\mathbf{P}}_a\\ \tilde{\mathbf{P}}_m\end{Bmatrix} = \begin{Bmatrix}\mathbf{F}_a\\ \mathbf{0}\end{Bmatrix} \tag{27}$$

The final system of equations can be solved for a given pressure field once the prescribed pressures have been applied. After solving Eq. (27), the transmission loss (TL) can be evaluated to study the acoustic performance of the dissipative muffler. This parameter is defined as the difference between the sound power incident on an acoustic filter and the sound power transmitted downstream considering an anechoic termination and can be calculated by [1]

$$\mathrm{TL} = 20\log_{10}\frac{P_{inc}}{P_{trans}} \tag{28}$$

where P_{inc} and P_{trans} are the incident and transmitted pressures, respectively.

2.2. Heterogeneous acoustic properties of the absorbent material

The acoustic behaviour of the absorbent materials considered in the literature can be described by the equivalent characteristic impedance $Z_m = \rho_m c_m$ and wavenumber $k_m = \omega/c_m$. These complex and frequency dependent properties have usually a constant value from a spatial point of view throughout the fibrous material domain, assuming a homogeneous steady airflow resistivity R [3, 4, 21]. The resistivity can be related to the filling density ρ_c by means of [26]

$$R = A_1{\rho_c}^{A_2} \tag{29}$$

where the values A_1 and A_2 are independent of the filling density and can be obtained, for a given absorbent material, by a least squares fitting from experimental data. For the absorbent material under consideration (Owens Corning's texturized Advantex fiber glass roving) the values $A_1 = 1.316074$ and $A_2 = 1.782163$ are taken into account [4, 27] with R and ρ_c in SI units.

Although ρ_c is usually assumed to be constant in the bibliography, strong heterogeneities can be found in practical applications. During the manufacturing process of automotive dissipative mufflers, meaningful variations in the filling density can be produced causing a change in the steady airflow resistivity of the absorbent material. Also, the flow of soot particles [17] can induce spatial modifications of the material properties. In this investigation, a coordinate-dependent linear function $\rho_c(x) = ax+b$ is assumed to simulate the variation of the filling density along the main axial direction of the muffler. Eq. (29) leads then to a coordinate-dependent resistivity $R(x)$, and a modified version of the homogeneous models of earlier studies [3, 4, 21, 27, 28] is obtained, where the characteristic impedance and wavenumber of the heterogeneous absorbent material are expressed as follows,

$$\frac{Z_m(x)}{Z_0} = \left[\left(1 + 0.09534\left(\frac{f\rho_0}{R(x)}\right)^{-0.754}\right) + j\left(-0.08504\left(\frac{f\rho_0}{R(x)}\right)^{-0.732}\right)\right] \tag{30}$$

$$\frac{k_m(x)}{k_0} = \left[\left(1 + 0.16\left(\frac{f\rho_0}{R(x)}\right)^{-0.577}\right) + j\left(-0.18897\left(\frac{f\rho_0}{R(x)}\right)^{-0.595}\right)\right] \tag{31}$$

with $Z_0 = \rho_0 c_0$ being the characteristic impedance of the air and f the frequency. Therefore, the introduction of spatial variations in the filling density leads finally to heterogeneity associated with R, Z_m and k_m.

2.3. Acoustic impedance of the perforated duct

As it was shown in the work of Kirby and Cummings [19], the acoustic impedance of the perforated duct in presence of homogeneous absorbent material strongly depends on the acoustic properties of the fibrous dissipative medium backing the perforations. In this investigation, the equivalent characteristic impedance Z_m and wavenumber k_m are coordinate-dependent and therefore the expression used in earlier works [3, 4] for the acoustic impedance of the perforations, has been redefined here to introduce the heterogeneity of the absorbent material, giving

$$\tilde{Z}_p(x) = Z_0 \frac{\left(0.006 + jk_0\left(t_p + 0.425d_h\left(1 + \frac{Z_m(x)}{Z_0}\frac{k_m(x)}{k_0}\right)F(\sigma)\right)\right)}{\sigma} \tag{32}$$

where d_h denotes the hole diameter, t_p the thickness, σ the porosity, and $F(\sigma)$ a factor that takes into account the interaction between perforations [29]. Here, $F(\sigma)$ is obtained as the average value of Ingard's and Fok's corrections, denoted $F_I(\sigma)$ and $F_F(\sigma)$, respectively. Ingard's function is given by

$$F_I(\sigma) = 1 - 0.7\sqrt{\sigma} \tag{33}$$

and Fok's correction is calculated as

$$F_F(\sigma) = 1 - 1.41\sqrt{\sigma} + 0.34\left(\sqrt{\sigma}\right)^3 + 0.07\left(\sqrt{\sigma}\right)^5 \tag{34}$$

2.4. Segmentation method

To validate the proposed finite element approach, a comparison between the results given by the implemented procedure and calculations obtained by a segmentation method is carried out. As can be seen in Figure 2, in this method [16, 30] the heterogeneous absorbent material is divided into N regions with lengths L_1, L_2, ..., L_N and the associated homogeneous filling densities are evaluated by

$$\tilde{\rho}_{c\,j} = \left(\rho_{c\,j} + \rho_{c\,j+1}\right)/2, \qquad \text{for } j = 1, 2, ..., N \tag{35}$$

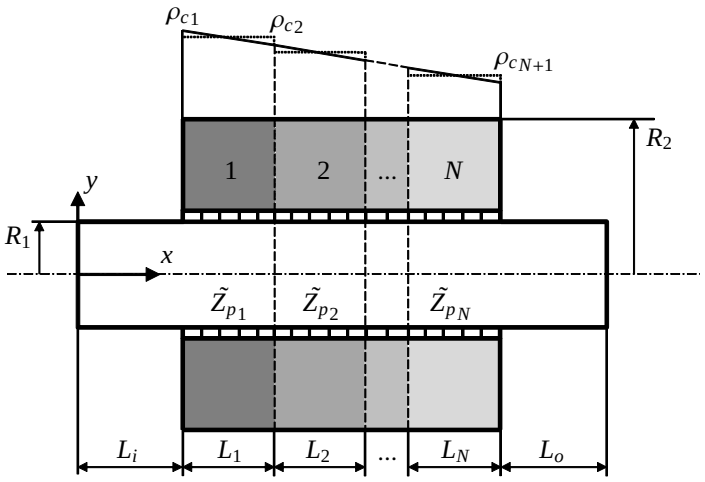

Figure 2: Sketch of the perforated dissipative silencer with heterogeneous absorbent material associated with the segmentation method.

After evaluating $\tilde{\rho}_{c\,j}$, the resistivity of each segment is given by Eq. (29). The equivalent complex density $\rho_{m\,j}$ and speed of sound $c_{m\,j}$ associated with segment j can be obtained from Eqs. (30) and (31). Similarly, the acoustic impedance of the perforated duct $\tilde{Z}_{p\,j}$ associated with region j can be calculated by Eq. (32). The results obtained by considering the segmentation procedure have been carried out by the finite element package LMS Virtual.Lab [31].

3. Results and discussion

3.1. Validation

Figure 3 shows the comparison of the transmission loss (TL) predictions obtained by the implemented procedure as well as those from the segmentation method. The muffler geometry is axisymmetric, and the dimensions of the studied configuration are: central passage radius $R_1 = 0.0245$ m, outer chamber radius $R_2 = 0.0822$ m, length of the inlet and outlet ducts $L_i = L_o = 0.1$ m and length of the absorbent material $L_m = 0.3$ m (see Figure 2). The perforated duct is characterized by a porosity $\sigma = 20\%$, thickness $t_p = 0.001$ m and hole diameter $d_h = 0.0035$ m. In the proposed approach for the heterogeneous absorbent materials, the filling density is assumed to vary according to the function $\rho_c(x) = -653.333x + 359.333$. This assumption provides a mean filling density of value $\rho_c = 196$ kg/m^3. For the segmentation

method calculations three cases have been computed with 1, 2 and 3 segments, considering a homogeneous absorbent material in each region. Therefore, the case with $N = 1$ corresponds to a perforated dissipative muffler with homogeneous absorbent material. The lengths of segments and the associated filling densities for the three cases are shown in Table 1. In the segmentation method predictions and the proposed approach results as well, the fibrous material total mass is constant with a value of 1.137 kg. The axisymmetric finite element mesh for the studied muffler consists of eight-noded quadratic quadrilateral elements with an approximate size of 0.01 m. For the maximum frequency of interest, 3200 Hz, the acoustic wavelength is about 0.1 m. Therefore the finite element mesh includes 10 elements per wavelength, which is sufficiently accurate for the transmission loss predictions. As can be seen in Figure 3, all the curves exhibit a reasonable agreement at low frequencies, where the attenuation of the muffler is mainly dictated by reactive phenomena [1]. In the mid and high frequency range, considerable differences between the implemented procedure results and the segmentation method predictions with 1 segment (homogeneous absorbent material) can be observed. At 1310 Hz the difference is about 10% (approximately 6 dB). By increasing the number of segments, the results provided by the segmentation approach exhibit a convergence to the proposed method and the discrepancies are gradually lower. For $N = 3$, some slight differences are still detected between the results obtained by the proposed approach and the segmentation procedure.

	Length (m)			Filling density $\left(\mathrm{kg/m^3}\right)$		
N	L_1	L_2	L_3	ρ_{c1}	ρ_{c2}	ρ_{c3}
1	0.30	–	–	196	–	–
2	0.15	0.15	–	245	147	–
3	0.10	0.10	0.10	261.3	196	130.7

Table 1: Lengths of the segments and the associated filling density.

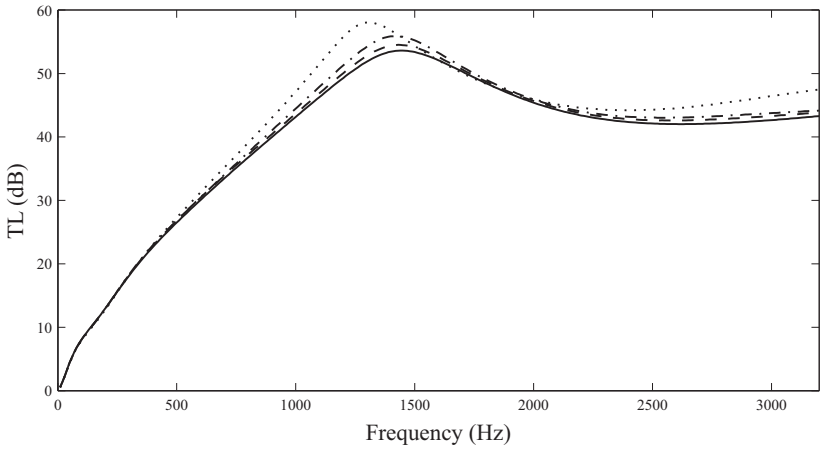

Figure 3: TL of perforated dissipative silencer: - - - -, segmentation method, $N = 1$; — · —, segmentation method, $N = 2$; — — —, segmentation method, $N = 3$; ———, implemented procedure.

3.2. *Effect of the filling density*

Figure 4 presents the effect of the filling density on the acoustic attenuation of perforated dissipative mufflers. The results have been obtained by applying the proposed approach presented in this work (heterogeneous material with continuously varying filling density) and the segmentation method with $N = 1$ as well (homogeneous absorbent material case). The values $\rho_c = 90$ kg/m^3, $\rho_c = 166.7$ kg/m^3 and $\rho_c = 196$ kg/m^3 are considered for the geometry analyzed in the previous figure. In the segmentation method calculations these values represent the constant filling densities within the outer dissipative chamber Ω_m, while in the implemented procedure they denote the mean filling densities. In this latter case, the axial distributions are given by $\rho_c(x) = -300x + 165$, $\rho_c(x) = -555.733x + 305.653$ and $\rho_c(x) = -653.333x + 359.333$, respectively. The perforated duct is characterized by $\sigma = 20\%$, $t_p = 0.001$ m and $d_h = 0.0035$ m. As can be observed in Figure 4, for all the considered filling densities, the transmission loss curves associated with the proposed approach (heterogeneous material) are clearly different from those obtained by the segmentation method (homogeneous material), even when the comparison is carried out with the same total mass of absorbent material. Therefore, the impact of the material heterogeneity on the sound attenuation is remarkable, which justifies the approach presented in the current investigation. As the filling density increases, the two approaches show higher discrepancies between them. Also, it can be seen that, with higher filling densities, the transmission loss predictions obtained by the two approaches are increased at mid to high frequencies, and the resonant peaks are shifted to lower frequencies. At very low frequencies, an opposite trend appears, that is, higher filling densities tend to reduce the acoustic attenuation.

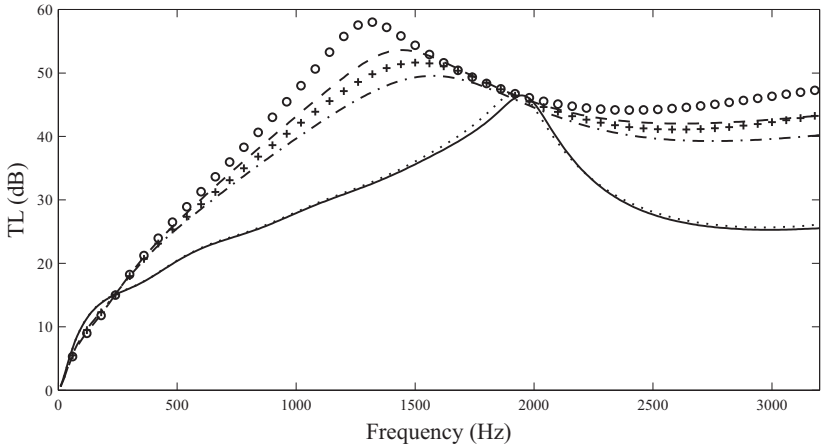

Figure 4: TL of perforated dissipative silencer: ———, $\rho_c = 90$ kg/m^3, heterogeneous material; - - - -, $\rho_c = 90$ kg/m^3, homogeneous material; — - —, $\rho_c = 166.7$ kg/m^3, heterogeneous material; + + +, $\rho_c = 166.7$ kg/m^3, homogeneous material; — — —, $\rho_c = 196$ kg/m^3, heterogeneous material; o o o, $\rho_c = 196$ kg/m^3, homogeneous material.

3.3. *Effect of the perforated duct porosity*

The influence of the perforated duct porosity is analyzed in Figure 5, where the values $\sigma = 5\%$, $\sigma = 10\%$ and $\sigma = 20\%$ have been considered while keeping $t_p = 0.001$ m and $d_h = 0.0035$ m. As in the latter case, the transmission loss curves have been obtained by applying the proposed approach as well as the segmentation method with $N = 1$ in order to assess the

impact of heterogeneities within the outer dissipative chamber. The absorbent material used for the calculations has a filling density ρ_c of 196 kg/m^3. This value is constant in the segmentation method (homogeneous material) and, for the heterogeneous one, provides the mean density in the implemented procedure. In this latter case (heterogeneous absorbent material) the axial variation of the filling density is defined by $\rho_c(x) = -653.333x + 359.333$. As can be seen, for all the considered porosities, the two approaches exhibit a reasonable agreement at low frequencies, while at mid to high frequencies significant discrepancies appear between them. For a particular porosity, these differences between the heterogeneous model and the homogeneous predictions over the frequency range considered in the computations can be associated with the influence of the material properties in the three-dimensional wave propagation. The influence of the material interacts with the acoustic behaviour of the perforated surface and the geometrical dimensions of the muffler, and therefore the sound attenuation phenomena are dictated by a high number of parameters. These complexities hinder a straightforward interpretation of all the details depicted in the attenuation curves. However, some clear general trends are found. Figure 5 shows that, by increasing the porosity of the perforated duct, the acoustic performance of the dissipative silencers is considerably improved at high frequencies since more sound attenuation is generated within the absorbent material. In addition, the resonant peaks are shifted to high frequencies due to the decrease of the mass reactance. At low frequencies, higher porosities lead to slightly lower transmission loss.

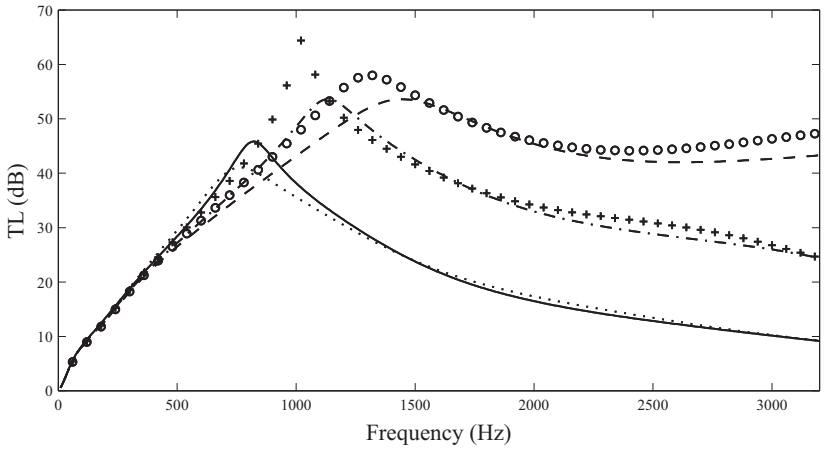

Figure 5: TL of perforated dissipative silencer: ———, σ = 5%, heterogeneous material; - - - -, σ = 5%, homogeneous material; — · — ·—, σ = 10%, heterogeneous material; + + +, σ = 10%, homogeneous material; — — —, σ = 20%, heterogeneous material; o o o, σ = 20%, homogeneous material.

4. Conclusions

A finite element approach has been developed to predict the acoustic behaviour of perforated dissipative mufflers with non-homogeneous properties. The heterogeneities of the absorbent material have been modelled by introducing a spatial variation of its filling density, that leads, through the steady airflow resistivity, to coordinate-dependent acoustic properties such as the equivalent complex density and the speed of sound. Therefore, the usual calculation of the finite

element matrices has been modified to include these equivalent heterogeneous acoustic properties. In addition, the coupling between the central passage and the dissipative outer chamber has been carried out considering a perforated surface. Since the acoustic impedance of the perforations in the presence of a backing porous medium strongly depends on the acoustic properties of the fibrous material, additional features have been implemented in comparison with the models of earlier studies. Specifically, the perforated acoustic impedance models normally used in the bibliography have been modified to introduce the spatial influence of the heterogeneous properties of the fibrous material.

To validate the numerical approach, the results provided by the proposed technique have been compared with a segmentation method that considers a sequence of homogeneous regions within the outer chamber, showing a good agreement for increasing number of segments. Although the calculations exhibit some discrepancies, particularly when a reduced number of regions is considered, a suitable convergence to the proposed approach has been found for the selected configuration under analysis as the number of segments increases. Finally, a study has been presented to assess the influence of the heterogeneity, the filling density and the porosity of the perforated duct on the sound attenuation of the dissipative mufflers.

5. Acknowledgments

The authors gratefully acknowledge the financial support of Ministerio de Ciencia e Innovación and the European Regional Development Fund by means of the projects DPI2007-62635 and DPI2010-15412.

6. References

[1] M. L. Munjal, Acoustics of Ducts and Mufflers, Wiley-Interscience, Nueva York, 1987.
[2] A. Selamet, M. B. Xu, I. J. Lee, N. T. Huff, Dissipative expansion chambers with two concentric layers of fibrous materials, International Journal of Vehicle Noise and Vibration 1 (2005) 341–357.
[3] F. D. Denia, A. G. Antebas, A. Selamet, A. M. Pedrosa, Acoustic characteristics of circular dissipative reversing chamber mufflers, Noise Control Engineering Journal 59 (2011) 234–246.
[4] F. D. Denia, A. Selamet, F. J. Fuenmayor, R. Kirby, Acoustic attenuation performance of perforated dissipative mufflers with empty inlet/outlet extensions, Journal of Sound and Vibration 302 (2007) 1000–1017.
[5] C. I. J. Young, M. J. Crocker, Prediction of transmission loss in mufflers by the finite element method, Journal of the Acoustical Society of America 57 (1975) 144–148.
[6] K. S. Peat, K. L. Rathi, A finite element analysis of the convected acoustic wave motion in dissipative silencers, Journal of Sound and Vibration 184 (1995) 529–545.
[7] T. W. Wu, Boundary Element Acoustics, WIT Press, Southampton, 2000.
[8] J. Galindo, J. R. Serrano, F. J. Arnau, P. Piqueras, High-frequency response of a calculation methodology for gas dynamics based on Independent Time Discretisation, Mathematical and Computer Modelling 50 (2009) 812–822.
[9] Z. L. Ji, Boundary element acoustic analysis of hybrid expansion chamber silencers with perforated facing, Engineering Analysis with Boundary Elements 34 (2010) 690–696.
[10] F. Piscaglia, A. Montorfano, G. Ferrari, G. Montenegro, High resolution central schemes for multi-dimensional non-linear acoustic simulation of silencers in internal combustion engines, Mathematical and Computer Modelling 54 (2011) 1720–1724.
[11] Y. Kagawa, T. Yamabuchi, A. Mori, Finite element simulation of an axisymmetric acoustic transmission system with a sound absorbing wall, Journal of Sound and Vibration 53 (1977) 357–374.
[12] A. Craggs, A finite element method for modelling dissipative mufflers with a locally reactive lining, Journal of Sound and Vibration 54 (1977) 285–296.
[13] R. Kirby, Transmission loss predictions for dissipative silencers of arbitrary cross section in the presence of mean flow, Journal of the Acoustical Society of America 114 (2003) 200–209.
[14] R. Kirby, A comparison between analytic and numerical methods for modelling automotive dissipative silencers with mean flow, Journal of Sound and Vibration 325 (2009) 565–582.

[15] T. Elnady, M. Åbom, S. Allam, Modeling perforates in mufflers using two-ports, Journal of Vibration and Acoustics 132 (2010) 1–11.
[16] A. Selamet, M. B. Xu, I. J. Lee, N. T. Huff, Effects of voids on the acoustics of perforated dissipative silencers, International Journal of Vehicle Noise and Vibration 2 (2006) 357–372.
[17] S. Allam, M. Åbom, Sound propagation in an array of narrow porous channels with application to diesel particulate filters, Journal of Sound and Vibration 291 (2006) 882–901.
[18] J. W. Sullivan, M. J. Crocker, Analysis of concentric-tube resonators having unpartitioned cavities, Journal of the Acoustical Society of America 64 (1978) 207–215.
[19] R. Kirby, A. Cummings, The impedance of perforated plates subjected to grazing gas flow and backed by porous media, Journal of Sound and Vibration 217 (1998) 619–636.
[20] I. J. Lee, A. Selamet, N. T. Huff, Acoustic impedance of perforations in contact with fibrous material, Journal of the Acoustical Society of America 119 (2006) 2785–2797.
[21] A. Selamet, M. B. Xu, I. J. Lee, N. T. Huff, Analytical approach for sound attenuation in perforated dissipative silencers, Journal of the Acoustical Society of America 115 (2004) 2091–2099.
[22] J. F. Allard, Propagation of Sound in Porous Media: Modelling Sound Absorbing Materials, Elsevier Science Publishers LTD, 1993.
[23] J. E. Murphy, S. A. Chin-Bing, A finite element model for ocean acoustic propagation and scattering, Journal of the Acoustical Society of America 86 (1989) 1478–1483.
[24] O. C. Zienkiewicz, R. L. Taylor, J. Z. Zhu, The Finite Element Method: Its Basis and Fundamentals, Elsevier Butterworth-Heinemann, 2005.
[25] R. Kirby, F. D. Denia, Analytic mode matching for a circular dissipative silencer containing mean flow and a perforated pipe, Journal of the Acoustical Society of America 122 (2007) 3471–3482.
[26] R. Kirby, A. Cummings, Prediction of the bulk acoustic properties of fibrous materials at low frequencies, Applied Acoustics 56 (1999) 101–125.
[27] A. Selamet, I. J. Lee, N. T. Huff, Acoustic attenuation of hybrid silencers, Journal of Sound and Vibration 262 (2003) 509–527.
[28] M. E. Delany, E. N. Bazley, Acoustical properties of fibrous absorbent materials, Applied Acoustics 3 (1970) 105–116.
[29] J. L. Bento, Acoustic characteristics of perforate liners in expansion chambers, Ph.D. thesis, University of Southampton (1983).
[30] F. D. Denia, A. G. Antebas, J. Martínez-Casas, F. J. Fuenmayor, Transmission loss calculations for dissipative mufflers with temperature gradients, in: Twentieth International Congress on Acoustics, Sydney, 2010.
[31] LMS International, LMSVirtual.Lab, Rev 7B (2007).